

Structures and Aggregation States of Fluoromethylithium and Chloromethylithium Carbenoids in the Gas Phase and in Ethereal Solvent

Lawrence M. Pratt*

Department of Chemistry, Fisk University, Nashville, Tennessee 37208

Bala Ramachandran

Departments of Chemistry and Physics, Louisiana Tech University, Ruston, Louisiana 71272

James D. Xidos, Christopher J. Cramer,* and Donald G. Truhlar*

Department of Chemistry and Supercomputer Institute, University of Minnesota, 207 Pleasant St. S.E., Minneapolis, Minnesota 55455-0431

lpratt@fisk.edu; cramer@chem.umn.edu; truhlar@chem.umn.edu

Received June 6, 2002

Using high-level quantum mechanical calculations and various models to account for solvation effects, monomers and dimers of fluoromethylithium and chloromethylithium carbenoids are studied in the gas phase and in dimethyl ether solvent. A combination of explicit microsolvation and a continuum reaction field is required to account fully for the structural and energetic effects of solvation. One important effect of solvent is the stabilization of charge-separated structures in which the lithium–halogen distance is much greater than in the gas-phase structures. At the most complete level of theory the 173 K standard-state free energy of dimerization of fluoromethylithium in dimethyl ether is predicted to be -0.9 kcal mol⁻¹, while that for chloromethylithium in the same solvent is predicted to be 3.7 kcal mol⁻¹. This suggests that, under typical experimental conditions, dimers of chloroalkyllithiums will not be observed, while dimers of fluoroalkyllithiums may contribute to the equilibrium population at a detectable level.

Introduction

Free carbenes may in principle be generated by the α -elimination of a lithium halide salt from a hydrocarbon precursor having the form R–C(Li)(X)–R'.^{1–6} The lithiated species may be generated either from the deprotonation of a haloalkane by an alkyllithium reagent (or suitably basic lithium alkoxide) or by lithium–halogen exchange at a doubly halogenated position. Lithium carbenoids have proven to be useful reagents in many synthetic transformations,^{1–7} including the generation of cyclopropane rings from olefin precursors,^{1–12} one-carbon

homologation of *B*-methoxyboracyclanes¹³ and boronic acids,¹⁴ synthesis of (chloromethyl)silanes,¹⁵ and generation of ketones from ester precursors.¹⁶ In many of these reactions, it is unclear whether the reactive species is the carbenoid, free carbene liberated from the carbenoid, or both.

Seebach and co-workers were able to demonstrate the existence of a number of halomethylithium carbenoids as stable, or at most slowly exchanging, compounds in tetrahydrofuran (THF) solutions at -100 °C based on NMR observation of ¹J(⁶Li, ¹³C) and ¹J(⁷Li, ¹³C) coupling constants.^{17–20} On the basis of the known strong coordination of tetramethylethylenediamine (TMEDA) to trichloromethylithium carbenoid,²¹ it has been suggested that the stability of the carbenoids observed in the NMR

(1) (a) Köbrich, G.; Akhtar, A.; Ansari, F.; Breckoff, W. E.; Büttner, H.; Drischel, W.; Fischer, R. H.; Flory, K.; Fröhlich, H.; Goyert, W.; Heinemann, H.; Hornke, I.; Merkle, H. R.; Trapp, H.; Zündorf, W. *Angew. Chem., Int. Ed. Engl.* **1967**, *1*, 41. (b) Gilchrist, T. L.; Rees, C. W. *Carbenes, Nitrenes, and Arynes*; Nelson: London, UK, 1969; p 85. (2) Kirmse, W. *Carbene Chemistry*, 2nd ed.; Academic Press: New York, 1971.

(3) Seyferth, D. In *Carbenes*; Moss, R. A., Jones, M., Eds.; Krieger: Malabar, FL, 1973; Vol. 2, p 101.

(4) Wentrup, C. *Reactive Molecules*; Wiley: New York, 1984; p 162.

(5) Moss, R. A.; Jones, M. In *Reactive Intermediates*; Jones, M., Moss, R. A., Eds.; John Wiley & Sons: New York, 1985; Vol. 3, p 45.

(6) March, J. *Advanced Organic Chemistry*, 4th ed.; John Wiley & Sons: New York, 1992; p 198.

(7) Marchand, A. P. In *The Chemistry of Double-Bonded Functional Groups*; Patai, S., Ed.; Wiley-Interscience: New York, 1977; Supplement A.

(8) Closs, G. L.; Closs, L. E. *Angew. Chem., Int. Ed. Engl.* **1962**, *1*, 334.

(9) Closs, G. L.; Moss, R. A. *J. Am. Chem. Soc.* **1964**, *86*, 4042.

(10) Krief, A. *Tetrahedron* **1980**, *36*, 2531.

(11) Siegel, H. *Top. Curr. Chem.* **1982**, *106*, 55.

(12) Taylor, K. G. *Tetrahedron* **1982**, *38*, 2752.

(13) Brown, H. C.; Phadke, A. S.; Rangaiashenvi, M. V. *J. Am. Chem. Soc.* **1988**, *110*, 6263.

(14) Sundararajan, R.; Li, G.; Brown, H. C. *Tetrahedron Lett.* **1994**, *35*, 8957.

(15) Kobayashi, T.; Pannell, K. H. *Organometallics* **1991**, *10*, 1960.

(16) Megia-Fernandez, E.; Sardina, F. J. *Tetrahedron Lett.* **1997**, *38*, 673.

(17) Seebach, D.; Siegel, H.; Muller, K.; Hiltbrunner, K. *Angew. Chem., Int. Ed. Engl.* **1979**, *18*, 784.

(18) Siegel, H.; Hiltbrunner, K.; Seebach, D. *Angew. Chem., Int. Ed. Engl.* **1979**, *18*, 785.

(19) Seebach, D.; Siegel, H.; Gabriel, J.; Hässig, R. *Helv. Chim. Acta* **1980**, *63*, 2046.

(20) Seebach, D.; Hässig, R.; Gabriel, J. *Helv. Chim. Acta* **1983**, *66*, 308.

(21) Köbrich, G. *Angew. Chem., Int. Ed. Engl.* **1972**, *11*, 473.

experiments might be dependent in part on strong coordination of solvent THF molecules to lithium.⁴

One area where the data were not conclusive was with respect to the aggregation state(s) of the species involved (e.g., monomer, dimer, or higher order aggregates). However, Seebach et al.²⁰ did report X-ray crystal structural data for the species 2-lithio-2-methyl-1,3-dithiane TMEDA solvate and 2-lithio-2-phenyl-1,3-dithiane TMEDA–THF mixed solvate, which might be expected to have some resemblance to halolithium carbenoids. The former compound was reported to have a dimeric chair-like structure, while the more sterically hindered phenyl derivative was reported to be monomeric. Both crystal structures showed ethereal ligands coordinated to the lithium atoms. Although there is no guarantee that any solid-state structure will coincide with the solution structure of the same compound, persistent strong coordination of polar solvent molecules to lithium cations in the liquid solution phase has been well-documented by NMR spectroscopy, kinetics, and computational methods.^{22–28}

With respect to prior computational work addressing lithium carbenoids and related structures, most has focused on isolated monomers.^{29–34} In addition, Rohde et al.³⁰ and Boche et al.³³ have computed data for a cyclic dimer of fluoromethyl lithium carbenoid at the HF/3-21G and MP2/6-31G* levels of theory, respectively. Solvation effects have not been considered in available calculations.

In this work, we apply high-level quantum chemical calculations to predict the gas-phase monomer–dimer equilibria for fluoromethyl lithium and chloromethyl lithium carbenoids (1-F and 1-Cl, respectively). In addition, we compute the influence of ethereal solvation on these equilibria, with special attention given to first-solvation shell phenomena in which the ethers directly coordinate to the Li centers.

Computational Methods

Gas Phase. All molecular geometries were fully optimized at several different levels of theory. Hybrid Hartree–Fock density-functional calculations making use of the *mPW1PW91* functional³⁵ were carried out with the following basis sets, listed in order of increasing completeness: MIDI!6D,^{36,37} 6-31+G(d),^{38–40} and MG3S. The MG3S basis is derived from

(22) Fraenkel, G.; Chow, A.; Winchester, W. R. *J. Am. Chem. Soc.* **1990**, *112*, 2582.

(23) Fraenkel, G.; Duncan, J. H.; Wang, J. H. *J. Am. Chem. Soc.* **1999**, *121*, 432.

(24) Fraenkel, G.; Duncan, J. H.; Martin, K.; Wang, J. *J. Am. Chem. Soc.* **1999**, *121*, 10538.

(25) Sun, X.; Collum, D. B. *J. Am. Chem. Soc.* **2000**, *122*, 2452.

(26) Sun, X.; Collum, D. B. *J. Am. Chem. Soc.* **2000**, *122*, 2459.

(27) Chadwick, S. T.; Rennels, R. A.; Rutherford, J. L.; Collum, D. B. *J. Am. Chem. Soc.* **2000**, *122*, 8640.

(28) Rutherford, J. L.; Collum, D. B. *J. Am. Chem. Soc.* **2001**, *123*, 199.

(29) Dill, J. D.; Schleyer, P. v. R.; Pople, J. A. *J. Am. Chem. Soc.* **1976**, *98*, 1663.

(30) Rohde, C.; Clark, T.; Kaufmann, E.; Schleyer, P. v. R. *J. Chem. Soc., Chem. Commun.* **1982**, 882.

(31) Mareda, J.; Rondan, N. G.; Houk, K. N. *J. Am. Chem. Soc.* **1983**, *105*, 6997.

(32) (a) Schleyer, P. v. R.; Clark, T.; Kos, A. J.; Spitznagel, G. W.; Rohde, C.; Arad, D.; Houk, K. N.; Rondan, N. G. *J. Am. Chem. Soc.* **1984**, *106*, 6467. (b) Wang, B.-Z.; Deng, C.-H.; Xu, L.-X.; Tao, F.-G. *Sci. China Ser. B* **1990**, *33*, 423.

(33) Boche, G.; Bosold, F.; Lohrenz, J. C. W.; Opel, A.; Zulauf, P. *Chem. Ber.* **1993**, *126*, 1873.

(34) Hermann, H.; Lohrenz, J. C. W.; Kühn, A.; Boche, G. *Tetrahedron* **2000**, *56*, 4109.

(35) Adamo, C.; Barone, V. *J. Chem. Phys.* **1998**, *108*, 664.

the MG3 basis⁴¹ by deleting diffuse functions on hydrogens. Note that *mPW1PW91* is the only density-functional-based computational level employed in this paper, and we will simply refer to this level of theory as DFT (the weaker performance of other functionals does not merit discussion). Optimizations were also carried out at the quadratic configuration interaction level including the effects of all single and double excitations (QCISD).⁴² The QCISD calculations employed the 6-31+G(d) basis set.

Vibrational frequency calculations were carried out to establish the nature of all optimized stationary points as minima. These calculations were also used to compute zero-point vibrational energies and vibrational and rotational thermal contributions to the enthalpy and free energy, using standard ideal-gas rigid-rotor harmonic-oscillator statistical mechanical approximations.⁴³ The standard state employed in free energy calculations was a concentration of 1 mol/L at 173 K. When monomers and/or dimers were found to exist as multiple conformers, free energies were computed as

$$\Delta G^\circ = -RT \ln \left(\sum_i e^{-\Delta G_i^\circ/RT} \right) \quad (1)$$

where ΔG_i° is the standard-state free energy of conformer *i*. This corresponds to summing the partition function over all accessible conformations, and free energies computed by eq 1 will be called conformationally inclusive.

In certain instances, single-point energy calculations were carried out at the DFT/MG3S and QCISD/MG3S levels with use of the DFT/MIDI!6D geometries. We employ standard nomenclature for these calculations, e.g., QCISD/MG3S//DFT/MIDI!6D.

Liquid Solution. All solvation calculations are based on dimethyl ether as solvent. Our most complete calculations include two explicit dimethyl ether molecules solvating each lithium cation, and they account for bulk solvation when a generalized Born (GB) reaction field formalism is used.⁴⁴ All of the parameters required for the GB calculations except the Coulomb radius of lithium were taken from the BPW91/MIDI!6D parametrization of Solvation Model 5.42R (SM5.42R).^{45,46} A Coulomb radius of 1.32 Å was chosen for lithium because, when used in the monatomic Born formula, this radius exactly reproduces the experimentally measured room temperature aqueous solvation free energy for lithium cation (−124 kcal/mol^{−1}).⁴⁷

Although SM5.42R models include both the bulk electrostatic and non-bulk-electrostatic components of the free energy of solvation, in this work we consider only the bulk electrostatic component, i.e., that derived from electric polarization of the solvent, electronic polarization of the solute, and geometric relaxation of the solute when that is allowed. When geometric relaxation in the liquid is not considered, the calculation is of the GBR-type where the “R” in the model name refers to a Rigid gas-phase geometry. When the geometry is allowed to

(36) Easton, R. E.; Giesen, D. J.; Welch, A.; Cramer, C. J.; Truhlar, D. G. *Theor. Chim. Acta* **1996**, *93*, 281.

(37) Thompson, J. D.; Winget, P.; Truhlar, D. G. *PhysChemComm* **2001**, 1.

(38) Hehre, W. J.; Ditchfield, R.; Pople, J. A. *J. Chem. Phys.* **1972**, *56*, 2257.

(39) Hariharan, P. C.; Pople, J. A. *Theor. Chim. Acta* **1973**, *28*, 213.

(40) Frisch, M. J.; Pople, J. A.; Binkley, J. S. *J. Chem. Phys.* **1984**, *80*, 3265.

(41) Fast, P. L.; Sanchez, M. L.; Truhlar, D. G. *Chem. Phys. Lett.* **1999**, *306*, 407.

(42) Pople, J. A.; Head-Gordon, M.; Raghavachari, K. *J. Chem. Phys.* **1987**, *87*, 5968.

(43) Cramer, C. J. *Essentials of Computational Chemistry: Theories and Models*; Wiley: Chichester, UK, 2002.

(44) Cramer, C. J.; Truhlar, D. G. *Chem. Rev.* **1999**, *99*, 2161.

(45) Zhu, T.; Li, J.; Hawkins, G. D.; Cramer, C. J.; Truhlar, D. G. *J. Chem. Phys.* **1998**, *109*, 9117.

(46) Li, J.; Zhu, T.; Hawkins, G. D.; Winget, P.; Liotard, D. A.; Cramer, C. J.; Truhlar, D. G. *Theor. Chem. Acc.* **1999**, *103*, 9.

(47) Noyes, R. M. *J. Am. Chem. Soc.* **1962**, *84*, 513.

relax in the liquid phase, the model is referred to simply as GB, i.e., the "R" is dropped from the model name. As we restrict our attention only to the bulk electrostatic component of the solvation free energy, the only solvent property that we require to accomplish the GB or GBR calculations is the bulk dielectric constant of dimethyl ether. Dimethyl ether has a dielectric constant of 10.144 at 173 K.⁴⁸

The free energy of a single conformer in solution is then taken to be the sum of its gas-phase free energy and its GB solvation free energy (using in both gaseous and liquid phases the same standard state of 1 mol/L and 173 K). Conformationally inclusive monomer and dimer free energies in solution are then computed according to eq 1.

All species considered in this paper are singlets. All energetic results are quoted on a molar basis.

Software. Calculations were performed with the Gaussian98⁴⁹ and MN-GSM⁵⁰ software packages.

Results and Discussion

This section is divided into two parts. We begin with an analysis of our most complete gas-phase and liquid-solution-phase calculations. In the gas phase, these are DFT/MG3S calculations. In solution we derive conformer free energies as the sum of DFT/MG3S//DFT/MIDI!6D gas-phase free energies for microsolvated species that include two dimethyl ether molecules coordinated to each lithium atom plus GB/DFT/MIDI!6D liquid-phase solvation free energies of the same microsolvated species. After this analysis, we briefly discuss certain technical issues that, inter alia, motivate the selection of the above levels as the most chemically useful ones.

Structures and energetics. In the gas phase, calculations at the DFT/MG3S level predict both the monomers and dimers of the two carbenoids to exist as single conformers (the monomers and dimers will be referred to as **1-F** and **1-Cl**, and **2-F** and **2-Cl**, respectively); these structures are shown in Figure 1. In the monomers, the carbon–halogen bond lengths are about 0.2 Å longer than those found for standard C–F and C–Cl bonds. Carbon–lithium bond lengths of just over 1.9 Å are predicted, suggesting some covalent interaction between the atoms. Upon dimerization, the lithium–halogen bond lengths do not change much, but the carbon–halogen bonds shorten while the carbon–lithium bonds lengthen. A lithium–lithium bond having a length of about 2.3 Å is predicted for the dimers.

Dimerization is predicted to be strongly exergonic in the gas phase. For **1-F** the free energy of dimerization is predicted to be –38.6 kcal, and for **1-Cl** the prediction is –33.4 kcal. To the extent that the carbenoids may be viewed as lithium cations coordinated to halomethylcar-

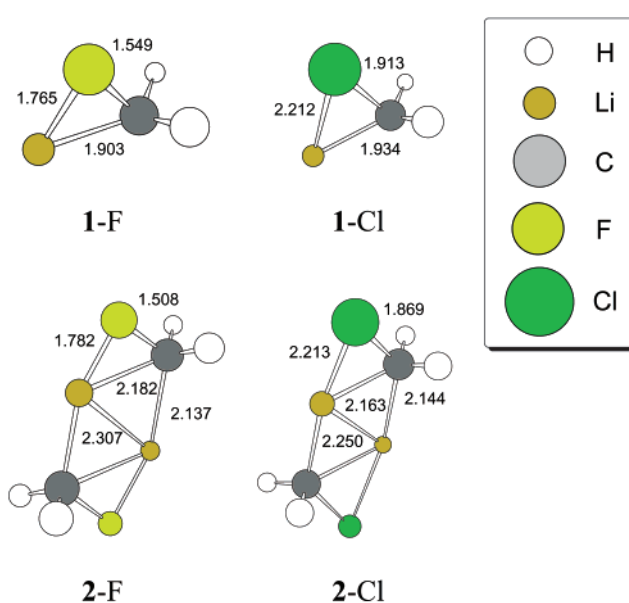


FIGURE 1. Monomer and dimer gas-phase stereostructures for fluoromethyl lithium and chloromethyl lithium carbenoids computed at the DFT/MG3S level; heavy-atom bond lengths (Å) are provided.

banions, there is clearly a strong ionic driving force reflected in the geometries of the dimers, although some covalent interaction between the lithium atoms also appears evident on the basis of these two atoms being closer than the sum of their van der Waals radii.

When two dimethyl ether molecules are allowed to coordinate to each lithium atom in gas-phase calculations at the DFT/MIDI!6D level (see below for details on validation of this lower level for geometry optimization) two monomer structures, **1a-F**·2S and **1b-F**·2S, are obtained for the fluoro case, and one, **1-Cl**·2S (where S = solvent), is obtained for the chloro case; see Figure 2. For the dimers, three different stereostructures are found for each halogen; see structures **2-F**·4S and **2-Cl**·4S in Figure 2. The existence of two different isomers for **1-F**·2S, one where fluorine is coordinated to lithium and one where it is not, but only one isomer of **1-Cl**·2S, which does not involve a Li–Cl interaction, appears to indicate that the Li–F interaction is in general stronger than a Li–Cl interaction, consistent with what would be expected on the basis of Li and F both being first-row elements.

Table 1 lists the relative energies of different isomers of microsolvated **1** and **2**, as well as the dimerization energies computed for the full population of all isomers at 173 K. The table also provides these data including the free energy of solvation computed using the generalized Born SCRF procedure for the cluster geometries, and for geometries fully relaxed with respect to solvation effects.

In the gas phase, the dimerization free energies for the microsolvated species are negative and large in magnitude, although they are significantly reduced compared to those for the bare carbenoids noted above. When the effects of bulk solvent are added by using the frozen gas-phase geometries, there are changes both in the relative energies of different isomers and in the overall dimerization energetics, with the latter change being larger than the former.

(48) *CRC Handbook of Chemistry and Physics*, 75th ed.; Lide, D. R., Ed.; CRC Press: Boca Raton, FL, 1995.

(49) Frisch, M. J.; Trucks, G. W.; Schlegel, H. B.; Scuseria, G. E.; Robb, M. A.; Cheeseman, J. R.; Zakrzewski, V. G.; Montgomery, J. A.; Stratmann, R. E.; Burant, J. C.; Dapprich, S.; Millam, J. M.; Daniels, A. D.; Kudin, K. N.; Strain, M. C.; Farkas, O.; Tomasi, J.; Barone, V.; Cossi, M.; Cammi, R.; Mennucci, B.; Pomelli, C.; Adamo, C.; Clifford, S.; Ochterski, J.; Petersson, G. A.; Ayala, P. Y.; Cui, Q.; Morokuma, K.; Malick, D. K.; Rabuck, A. D.; Raghavachari, K.; Foresman, J. B.; Cioslowski, J.; Ortiz, J. V.; Stefanov, B. B.; Liu, G.; Liashenko, A.; Piskorz, P.; Komaromi, I.; Gomperts, R.; Martin, R. L.; Fox, D. J.; Keith, T.; Al-Laham, M. A.; Peng, C. Y.; Nanayakkara, A.; Gonzalez, C.; Challacombe, M.; Gill, P. M. W.; Johnson, B. G.; Chen, W.; Wong, M. W.; Andres, J. L.; Head-Gordon, M.; Replogle, E. S.; Pople, J. A. *Gaussian98* (revision A.9); Gaussian, Inc.: Pittsburgh, PA, 1998.

(50) Xidos, J. D.; Li, J.; Hawkins, G. D.; Winget, P. D.; Zhu, T.; Rinaldi, D.; Liotard, D. A.; Cramer, C. J.; Truhlar, D. G.; Frisch, M. J. *mn-gsm* (version 99.7); University of Minnesota: Minneapolis, MN, 2001.

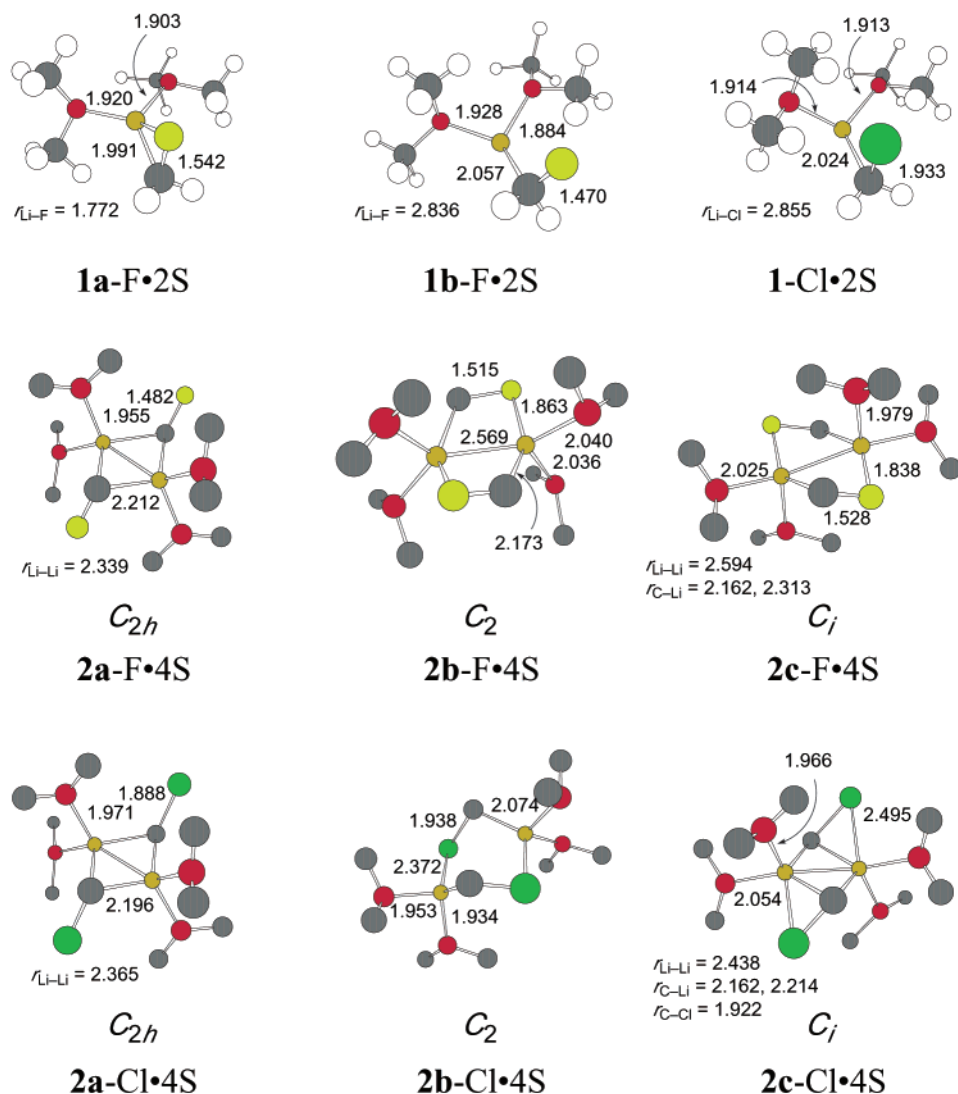


FIGURE 2. Microsolvated monomer and dimer gas-phase stereostructures for fluoromethyl lithium and chloromethyl lithium carbenoids computed at the DFT/MIDI!6D level; molecular point groups and heavy-atom bond lengths (Å) are provided. For clarity, hydrogen atoms are not shown in the dimers. See legend to Figure 1 for other atoms.

TABLE 1. Relative Free Energies and Free Energies of Dimerization (173 K, kcal mol⁻¹) for Conformers of 1-X•2S and 2-X•4S in the Gas Phase and in Methyl Ether Solution and the Conformationally Inclusive Standard-State Free Energy of Dimerization

X	level ^a	1a-X•2S	1b-X•2S	2a-X•4S	2b-X•4S	2c-X•4S	ΔG° dimerization ^b
F	DFT	0.0	3.1	4.1	0.0	0.4	-14.2
	GBR/DFT	0.0	-0.1	3.9	0.0	0.5	-2.7
	GB/DFT	0.0	0.2	3.8	0.0	0.2	-0.9
Cl	DFT	<i>c</i>	<i>c</i>	0.0	3.0	-0.5	-11.3
	GBR/DFT	<i>c</i>	<i>c</i>	0.0	0.4	1.7	-2.1
	GB/DFT	<i>c</i>	<i>c</i>	0.0	-0.4	1.7	3.7

^a DFT = DFT/MG3S//DFT/MIDI!6D with thermal contributions to free energy computed at the DFT/MIDI!6D level. GBR/DFT implies adding solvation free energies at gas-phase geometries. GB/DFT implies adding solvation free energies computed by allowing the microsolvated structures to fully relax in response to the continuum solvation reaction field. ^b Including the full population of isomers using eq 1 for each set. ^c Only a single isomer of 1-Cl•2S is predicted.

The relative energies of isomers **2-F•4S** do not show much sensitivity to solvation, but **1b-F•2S** is stabilized relative to **1a-F•2S** by 3.2 kcal. The more obtuse Li-C-F angle in **1b-F•2S** compared to **1a-F•2S** increases the overall charge separation between the electropositive lithium atom and the electronegative fluorine atom, so the observed change is in the expected direction, with

the species having more charge separation being better solvated. The isomers of **2-Cl•4S** also show significant sensitivity to solvation effects, with **2b-Cl•4S** being best solvated and **2c-Cl•4S** least. This ordering is again easily rationalized on the basis of molecular polarity. Isomer **2b-Cl•4S** is the only one with a permanent electric dipole moment (the other two isomers have centers of inversion

and thus zero dipole moments by symmetry) and moreover has the greatest exposure of the most polar atoms to bulk solvent. Isomer **2c-Cl-4S** has the least charge separation in the sense that the lithium and chlorine atoms are directly bonded and the overall structure is very compact.

While the differential solvation energies of the stereoisomers are interesting, a more important effect is that, irrespective of isomer, the net dimerization free energy becomes significantly less negative or even positive when bulk solvation effects are included. Since dimerization significantly reduces the exposure of the lithium and halogen atoms to bulk solvent, this effect is in the expected direction. Interestingly, although geometric relaxation in solution does not much change the isomeric relative energies compared to those computed with frozen geometries, it *does* uniformly improve the solvation of the monomers compared to the dimers. Thus, at the GB/DFT level, which is the most complete level in the present study, the dimerization free energies in solution for **1-F** and **1-Cl** are computed to be -0.9 and 3.7 kcal, respectively.

To better understand the impact of these computed free energies on experiment, it is instructive to consider the corresponding equilibrium constant for the dimerization process



where the equilibrium constant K is computed as

$$K = \frac{[\text{dimer}]}{[\text{monomer}]^2} = e^{-\Delta G^\circ/RT} \quad (3)$$

An interesting question is then to ask, given K , what initial monomer starting concentration c_0 will lead to an equilibrium where monomer and dimer are found at equal concentration (that concentration being $c_0/3$). That is, we seek the solution of

$$\frac{[c_0/3]}{[c_0/3]^2} = e^{-\Delta G^\circ/RT} \quad (4)$$

Given dimerization free energies of -0.9 and 3.7 kcal, we may compute c_0 values of 0.22 M and 1.5×10^5 M for fluoromethylithium carbenoid and chloromethylithium carbenoid, respectively. The former concentration is in the range of typical experimental solution concentrations, while the latter clearly cannot be achieved. Thus, mixtures of monomers and dimers in dimethyl ether may well be observable for fluoromethylithium carbenoid but not for chloromethylithium carbenoid.

It is worth noting that the difference between the fluoro and chloro cases is essentially entirely a gas-phase effect, i.e., it is intrinsic to the molecules themselves and not a manifestation of differential solvation effects on the dimerization process. Thus, in the gas phase dimerization of **1-F** is favored over that for **1-Cl** by 5.2 kcal, and the difference after accounting for microsolvation (inner-shell coordination at Li) and bulk solvation is a very similar 4.6 kcal. The more favorable dimerization energies predicted for the F compounds compared to those for the Cl compounds presumably reflect the stronger interactions expected between Li and F compared to Li and Cl, and thus we expect this effect to be general, i.e., any

carbenoid—dimerization will be more favorable in fluoro-substituted cases than chloro ones.

With that point in mind, it seems unlikely that chloro-substituted dimers will ever be observed. To the extent that our modeling has considered the smallest possible carbenoid, it seems likely that steric effects will tend to reduce gas-phase free energies of dimerization relative to the one-carbon system, so that larger initial concentrations of monomer will be required for dimer to be formed at observable concentrations. Such concentrations may be accessible with fluoroalkyllithium carbenoids, but are already out of range for the chloro case.

Technical Modeling Details. To assess the quality of the *mPW1PW91* functional, we compared that level of theory to QCISD, the latter being a post-Hartree–Fock molecular-orbital-theory method of well-established accuracy for a wide variety of problems.⁴³ As the QCISD model is considerably more demanding of resources, the largest basis set for which such a comparison was carried out was the 6-31+G(d) basis. Comparing optimized geometries from DFT/6-31+G(d) and QCISD/6-31+G(d), the average absolute difference in all heavy atom bond lengths in **1-F**, **1-Cl**, **2-F**, and **2-Cl** was 0.028 Å. Since several of these bonds are long and characterized by weak force constants, we consider this to be quite good agreement. Further validation of the methods is carried out by comparing total dimerization free energies from the two levels (with thermal contributions computed at the same level used for geometry optimization). For the F and Cl cases, the DFT/6-31+G(d) predictions are -40.6 and -34.3 kcal, respectively, while at the QCISD/6-31+G(d) level, these predictions are -41.0 and -37.4 kcal, respectively, which is acceptable agreement.

The somewhat larger discrepancy between DFT and QCISD for the chlorocarbenoid is in part associated with larger geometric differences predicted for that case. When DFT/MIDI!6D geometries are used, single-point calculations at the DFT/MG3S and QCISD/MG3S levels predict F dimerization energies of -38.5 and -39.2 kcal, respectively, and Cl dimerization energies of -33.4 and -31.9 kcal, respectively. Thus, with a common geometry, the agreement between the two levels improves to 1.5 kcal. The use of a larger basis set in the single-point calculations may also provide some improved agreement, since the calculations converge with different rates as the basis set is made more complete.

The above considerations suggest that the DFT/MG3S level should be very accurate for the isolated gas-phase species, but it is not practical to use the very large MG3S basis set for geometry optimizations of the microsolvated species, where many more heavy atoms are involved. We therefore examined the utility of a smaller basis set, namely MIDI!6D, for this purpose. When DFT/MG3S single-point calculations were carried out at the DFT/MIDI!6D geometries for **1-F** and **1-Cl**, the absolute energies were found to be only 1.0 and 0.6 kcal higher than for the structures fully optimized at the DFT/MG3S level. The excellent quality of geometries predicted by the MIDI!6D basis set in this test motivated us to use such geometries for the larger microsolvated species, with energy evaluations then being carried out as single-point calculations using the more complete basis set.

We turn now to some consideration of the importance of explicit microsolvation from a modeling perspective. Comparing Figure 1 to Figure 2, it is clear that micro-

solvation has a profound effect on molecular structures. In the monomers, it is responsible for the development of a new minimum energy structure on the potential energy surface with an obtuse X–C–Li angle (and, in the case of **1-Cl**, the acute minimum disappears altogether). Note that the Li–F bond distance in **1b-F**·2S is 1.07 Å greater than that in **1-F**. In the case of the dimers, the addition of two solvent molecules to each lithium atom effectively causes the breaking of at least one of the bonds between lithium and some other atom previously present in the gas-phase structures of **2**; this causes opening and puckering of these otherwise very compact gas-phase dimers. Given such a large effect from the first solvation shell acting in the capacity of a set of coordinating ligands, it is of interest to ask about the degree to which a pure continuum model can mimic these effects. Thus, we carried out GBR calculations on the nonmicro-solvated monomer and dimers and found that the dimerization free energies for **1-F** and **1-Cl** at the GBR/DFT level are predicted to be –5.4 and –10.3 kcal, respectively. This is rather poor agreement with the data predicted for the microsolvated structures (Table 1), but it must be recognized that the latter structures have been allowed to relax in geometry as a function of microsolvation, while the gas-phase nonmicro-solvated ones have not. Thus, a more fair comparison is to compare fully relaxed GB/DFT results for the two cases. At the GB/DFT level, the **1-F** and **1-Cl** dimerization free energies are predicted to be –2.9 and 5.9 kcal, respectively, in surprisingly good agreement with the corresponding microsolvated values of –0.9 and 3.7 kcal, respectively.

With respect to the geometric changes that take place upon relaxing the geometries in solution, there is a systematic tendency for all Li–halogen bonds to increase in length, particularly for nonmicro-solvated structures. Bonds from carbon to lithium also tend to lengthen, while carbon–halogen and Li–O bonds shrink. The magnitude of these bond length changes typically ranges from a few thousandths of an angstrom to a few tenths. The analogue of Figure 2 with relaxed heavy-atom bond lengths in solution is provided as Supporting Information.

An important point is that, although microsolvation appears to be more physically realistic, it can introduce methodological challenges. One challenge is that free energy must be computed by summing the partition function over a potentially rather large number of structural isomers. While we have performed a reasonably careful search (albeit not via an exhaustive, stochastic process) for additional isomers, it is conceivable that low-symmetry structures exist that we simply failed to locate. A separate issue is that microsolvated structures tend to become increasingly “floppy” with increased microsolvation, for example, one tetramicro-solvated dimer has 15 vibrational frequencies under 100 cm^{–1}. Normal modes characterized by very small vibrational frequencies, e.g., below 15 cm^{–1}, if treated in the standard fashion as quantum mechanical harmonic oscillators, may make very large contributions to the molecular partition function, and this can give rise to anomalously negative free energies.^{43,51} In principle, one can handle these low-frequency modes in a more rigorous fashion,^{51–54} but current approaches are still subject to potentially large

errors or are too expensive for molecules of the size under consideration here. To evaluate the possible influence of this issue on our computed dimerization free energies, we first note that $G = H - TS$ (where H , T , and S are enthalpy, temperature, and entropy, respectively), and the harmonic approximation breaks down more severely for the TS term than for H . Therefore, we computed hybrid dimerization energies that consist of adding differential solvation free energies to gas-phase *enthalpies* of dimerization to which we added the thermal contribution from the translational partition function. This yields an approximate free energy of dimerization that includes all enthalpic contributions plus the entropy of translation, solvation, and multiple conformations but excludes vibrational and rotational entropy. For the microsolvated cases, these F and Cl dimerization free energies are –0.1 and 5.8 kcal, respectively. The agreement with the full free energy in the fluoro case is within 1 kcal, which suggests errors due to vibrational entropy are no larger in magnitude than those introduced by other model approximations. In the chloro case, the disagreement is a more substantial 2.1 kcal; this introduces additional uncertainty, but from a practical standpoint, the deviation is in the direction of favoring monomer still more, so the effect on the conclusion that dimer is unlikely to be observed in actual experimental systems is unchanged.

Concluding Remarks

Organolithium compounds may exist in various aggregation states, and different aggregates may exhibit different properties and reactivities. (For example, the thermodynamics of dissociation of carbenoids to produce free carbene depends on the state of aggregation.³⁰) Solvent molecules may be strongly coordinated, and it is essential to include this effect in realistic models of their structure and reactivity. (For example, a recent study of the reactions of MeLi in dimer and trimer aggregates found different mechanisms in different solvents.⁵⁵) In the present study of lithium carbenoids, we found that ethereal solvent dramatically stabilizes charge-separated structures, so that liquid-phase and even microsolvated structures are much more open with respect to lithium–halogen distances than are the gas-phase structures. The lithium–carbon distances also tend to increase. Furthermore, solvation inhibits dimerization. As a result, we anticipate that chloromethyl lithium carbenoids exist almost exclusively as monomers in dimethyl ether, and we predict that fluoromethyl lithium carbenoids exist primarily as monomers at concentrations below 0.2 M.

Acknowledgment. This work was supported in part by the National Science Foundation under grant Nos. CHE0203346 (C.J.C.) and CHE00-92019 (D.G.T.).

Supporting Information Available: The analogue of Figure 2 for liquid-optimized structures, together with Cartesian coordinates for all structures. This material is available free of charge via the Internet at <http://pubs.acs.org>.

JO026022G

(52) Pitzer, K. S. *Quantum Chemistry*; Prentice Hall: Englewood Cliffs, NJ, 1953.

(53) Chuang, Y.-Y.; Truhlar, D. G. *J. Chem. Phys.* **2000**, *112*, 1221.

(54) Mielke, S. L.; Truhlar, D. G. *J. Chem. Phys.* **2001**, *114*, 621.

(55) Haffner, F.; Sun, C.; Williard, P. G. *J. Am. Chem. Soc.* **2000**, *122*, 12542.

(51) Mayer, S. W.; Schieler, L.; Johnston, H. S. *J. Chem. Phys.* **1966**, *45*, 385.